# Evaluation of Perfusion Quantification Methods with Ultrasound Contrast Agents in a Machine-Perfused Pig Liver

## Bewertung der Methoden zur Quantifizierung der Perfusion mittels Ultraschallkontrastmittel bei maschineller Perfusion einer Schweineleber

**Authors** M. Averkiou[1], C. P. Keravnou[2], M. L. Izamis[2], E. Leen[3]

**Affiliations**
[1] Bioengineering, University of Washington, Seattle, United States
[2] Mechanical and Manufacturing Engineering, University of Cyprus, Nicosia, Cyprus
[3] Hammersmith Hospital, Imperial College London, United Kingdom of Great Britain and Northern Ireland

**Key words**
- DCEUS quantification
- ex-vivo pig liver
- machine perfusion
- liver flow rate
- therapy monitoring

## Abstract

**Purpose:** To evaluate dynamic contrast-enhanced ultrasound (DCEUS) as a tool for measuring blood flow in the macro- and microcirculation of an ex-vivo machine-perfused pig liver and to confirm the ability of DCEUS to accurately detect induced flow rate changes so that it could then be used clinically for monitoring flow changes in liver tumors.

**Materials and Methods:** Bolus injections of contrast agents in the hepatic artery (HA) and portal vein (PV) were administered to 3 machine-perfused pig livers. Flow changes were induced by the pump of the machine perfusion system. The induced flow rates were of clinical relevance (150 – 400 ml/min for HA and 400 – 1400 ml/min for PV). Quantification parameters from time-intensity curves [rise time (RT), mean transit time (MTT), area under the curve (AUC) and peak intensity (PI)] were extracted in order to evaluate whether the induced flow changes were reflected in these parameters.

**Results:** A linear relationship between the image intensity and the microbubble concentration was confirmed first, while time parameters (RT and MMT) were found to be independent of concentration. The induced flow changes which propagated from the larger vessels to the parenchyma were reflected in the quantification parameters. Specifically, RT, MTT and AUC correlated with flow rate changes.

**Conclusion** Machine-perfused pig liver is an excellent test bed for DCEUS quantification approaches for the study of the hepatic vascular networks. DCEUS quantification parameters (RT, MTT, and AUC) can measure relative flow changes of about 20 % and above in the liver vasculature. DCEUS quantification is a promising tool for real-time monitoring of the vascular network of tumors.

**received** 1.9.2015
**accepted** 17.2.2016

**Bibliography**
**DOI** http://dx.doi.org/10.1055/s-0042-104645
Published online: 2016
Ultraschall in Med © Georg Thieme Verlag KG Stuttgart · New York · ISSN 0172-4614

**Correspondence**
***Prof. Michalakis Averkiou***
Bioengineering, University of Washington
Box 355061
98195-5061 Seattle
United States
Tel.: ++ 1/2 06/6 16 95 58
Fax: ++ 1/2 06/6 85 33 00
maverk@uw.edu

## Zusammenfassung

**Ziel:** Die Bewertung der dynamischen kontrastverstärkten Sonografie (DCEUS) als Methode zur Messung des Blutflusses in der Makro- und Mikrozirkulation einer Ex-Vivo maschinellen Perfusion einer Schweineleber. Bestätigung, dass DCEUS in der Lage ist, die induzierten Veränderungen der Flussrate exakt nachzuweisen und somit in der Klinik zur Überwachung von Flussveränderungen in Lebertumoren eingesetzt werden kann.

**Material und Methoden:** Bolus-Injektionen der Kontrastmittel in die Leberarterie (HA) und die Pfortader (PV) wurden an 3 Schweinelebern mit maschineller Perfusion verabreicht. Die Flussänderungen wurden durch die Pumpe des maschinellen Perfusionssystems verursacht. Die induzierten Flussraten waren klinisch relevant (150 – 400 ml/min für HA und 400 – 1400 ml/min für PV). Die Quantifizierungsparameter aus den Zeit-Intensitätskurven [Anstiegszeit (RT), mittlere Laufzeit (MTT), Fläche unter der Kurve (AUC) und Spitzenintensität (PI)] wurden extrahiert, um zu bewerten, ob die induzierten Flussänderungen von diesen Parametern widergespiegelt wurden.

**Ergebnisse:** Eine lineare Beziehung zwischen der Bildintensität und der Konzentration der Mikrobläschen wurde zuerst bestätigt, während die Zeitparameter (RT und MMT) unabhängig von der Konzentration gezeigt wurden. Die induzierten Flussänderungen, die sich von den größeren Gefäßen zum Parenchym verbreiten, werden durch die Quantifizierungsparameter reflektiert. Insbesondere die Parameter RT, MTT und AUC korrelierten mit Veränderungen der Flussrate.

**Schlussfolgerung:** Die maschinelle Perfusion der Schweineleber ist ein hervorragendes Testsystem für den DCEUS-Quantifizierungsansatz bei der Untersuchung des Lebergefäßsystems. Die DCEUS-Quantifizierungsparameter (RT, MTT und AUC) können die relativen Flussänderungen in etwa 20 % und mehr im Gefäßsystem der

Leber messen. Die DCEUS-Quantifizierung ist eine vielversprechende Methode für die Echtzeitüberwachung des Gefäßsystems von Tumoren.

## Introduction

Ultrasound contrast agents (UCA) are microbubbles that due to their size (1 – 10 µm) stay strictly in the circulation. Dynamic contrast-enhanced ultrasound (DCEUS) utilizes nonlinear imaging techniques to enable real-time visualization of blood flow in the macro- and micro-circulation [1, 2], and has provided improvements in the detection and characterization of tumors and paved the way for the evaluation of tumor angiogenesis [3].

Beyond qualitative assessment and diagnosis in oncology, DCEUS may play a role in disease staging and therapy monitoring by offering quantitative evaluation of tissue, organ, and tumor perfusion [3 – 6]. Time-intensity curves (TICs) are obtained by placing a region of interest (ROI) on a contrast image. Depending on the protocol of contrast agent administration (bolus or constant infusion [3, 6]), different mathematical models [7] derived from the indicator dilution theory [8] can be fitted to TICs to analytically extract important DCEUS quantification parameters such as the rise time (*RT*), the mean transit time (*MTT*), peak intensity (PI) and the area under the TIC curve (*AUC*). The underlying hypothesis is that these quantification parameters are sensitive to changes in blood flow caused by tumor growth or anti-angiogenic therapies [4 – 6].

DCEUS quantification methods have been studied in-vitro using flow tissue phantoms, typically constructed from tubing of various sizes to facilitate flow [9 – 11]. In-vitro studies have, however, limited physiological relevance since they represent a single passage of contrast through simple tubing, thereby ignoring the dispersion of microbubbles through branching vessels, variable flow resistance, and variable flow states.

Clinical trials have been performed [4, 12 – 16] in order to assess the ability of DCEUS quantification to predict patient response to drugs targeting angiogenesis. The extracted quantification parameters were correlated with the response evaluation criteria in solid tumors (RECIST) and overall survival, both currently used in clinics as the approved metrics for therapy evaluation [3, 6]. However, in addition to the difficulty measuring flow in the tumors due to their complex vasculature, other problems exist: lack of large and thorough reproducibility study [6, 17], conflicting views as to which quantification parameters best correlate with flow changes (AUC in [12, 15, 16], RT in [4] and PI in [14]), and variations in machine settings between sessions [6, 18, 19]. In a review article by a group of experts in the field [6], it is clearly stated that DCEUS quantification is still far from consensus and clinical use. In a guidelines article [3] the variations between quantification software are pointed out and the reproducibility is described as “acceptable” but further investigation is needed.

Recently, Izamis et al. [20] developed and evaluated a sub-normothermic human-sized machine perfusion system suitable to preserve slaughterhouse pig livers. They showed with biochemical and hemodynamic measurements and DCEUS imaging that the developed model is a simple, cost-effective approach for stable, ex-vivo whole organ preservation. To overcome the limitations of DCEUS quantification listed above, and to avoid costly and complex in-vivo animal experiments and ethical issues in clinical trials, we propose the use of the machine-perfused pig liver model as perfusion quantification development and validation test bed.

In the present study, machine-perfused pig livers were used to investigate bolus kinetics of contrast microbubbles in an environment which closely resembles in-vivo conditions. The effect of bubble concentration on bolus kinetics parameters was examined first. Then, various flow changes with clinical/physiological relevance were induced in the machine-perfused liver and were measured in the liver vasculature with DCEUS quantification. The quantification parameters (*RT*, *MTT*, *PI*, *AUC*) were evaluated for their ability to detect the induced flow changes in the liver vasculature. The accuracy, resolution, and limitations of DCEUS flow quantification were studied in an effort to understand its strengths and weaknesses when used clinically for real-time monitoring of the vascular network of tumors.

## Materials and Methods

### Indicator dilution theory

The wash-in and washout of contrast microbubbles in an ROI may be modeled by the indicator dilution theory [3, 8]. If the amount of indicator $m$ in a bolus injection is known and the indicator concentration as a function of time $c(t)$ is measured in an ROI, the volumetric blood flow ($Q$) and the blood volume ($V$) can be calculated in terms of *AUC* and *MTT*:

$$Q = m \cdot (AUC)^{-1} \quad (1)$$

$$V = Q \cdot MTT \quad (2)$$

where

$$AUC = \int_0^\infty c(t)dt \quad (3)$$

$$MTT = \frac{\int_0^\infty tc(t)dt}{\int_0^\infty c(t)dt} \quad (4)$$

Microbubble concentration cannot be measured directly, thus the backscattered intensity $I(t)$ is measured instead. Since intensity is linearly proportional to the concentration [9, 21], Eqs. (1) & (2) can be used to calculate Q and V from *AUC* and *MTT*. Here we also note that the rise time (*RT*) is linearly related to *MTT* (see Eq. (10) in the study by Strouthos et al. [7]) and hence to flow rate.

### Ex-vivo machine-perfused livers

The studies were approved by the Cyprus National Bioethics Committee and the National Veterinary Services. Three healthy porcine livers were procured from a local abattoir. Details on liver procurement and the perfusion system can be found elsewhere [20]. The organs were then stored on ice and transported to the laboratory (time of static cold storage was ≤ 1 hour), where they were connected to the machine perfusion system (**Fig. 1a**) and sustained for up to 3 hours.

Flow rate (produced with a peristaltic pump) was typically set to 800 ml/min for the portal vein (PV) and 400 ml/min for the hepatic artery (HA). The selected flow rates ensured that PV pressure was ≤ 10 $cmH_2O$ and HA pressure was between 60 and 100 $cmH_2O$, values similar to those of humans. Hepatic stability was ascertained with half-hour interval measurements of bile production, oxygen consumption, and sustained vascular perfusion. The perfusion was monitored via DCEUS imaging (**Fig. 2**). Typical images of a bolus injection administered to the liver are shown in **Fig. 2**.

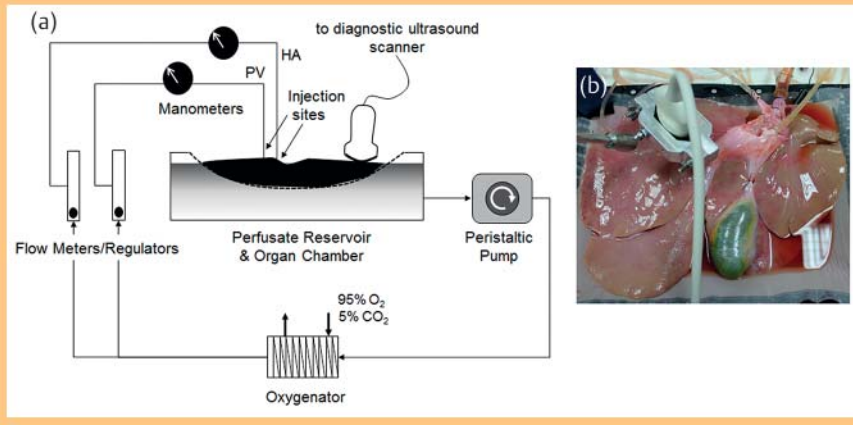


**Fig. 1** **a** The ex-vivo machine perfusion system consists of an organ chamber in which the liver is suspended, a single pump and oxygenator, and two flow meters/regulators connected to the hepatic artery and portal vein. **b** Picture of the pig liver connected to the machine perfusion system and the L9 – 3 imaging probe fixed at a specific location.

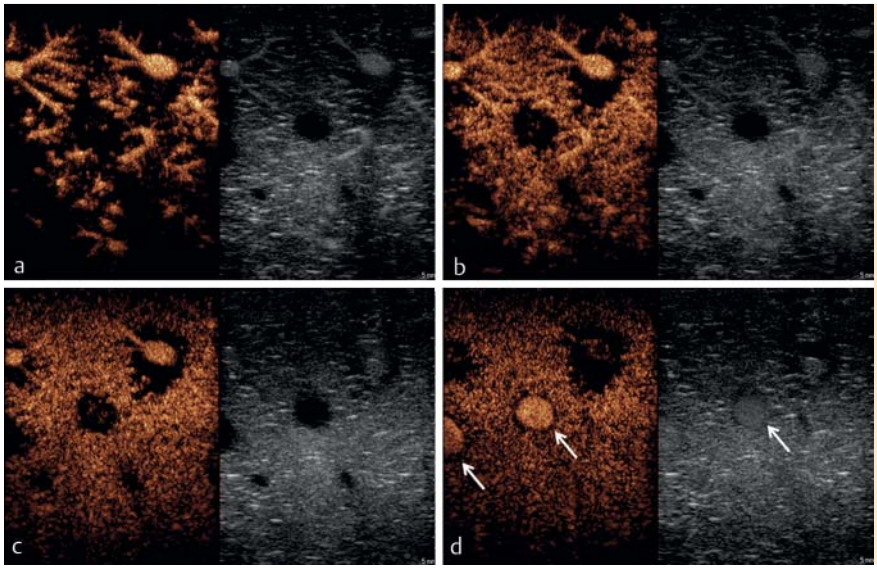


**Fig. 2** Images of microbubbles in the liver vasculature in a dual imaging mode where the left is the contrast image and the right is the tissue image. Flow in the vasculature of the liver can be depicted with administration of a contrast agent bolus directly into the portal vein (PV) or the hepatic artery (HA). A PV injection is used in this example. **a** First the primary branches are filled. **b, c** Contrast microbubbles enter the smallest capillaries and fill the parenchyma. **d** The contrast microbubbles appear in the hepatic vein (white arrows).

## Imaging

L12 – 5 and L9 – 3 linear array probes of an iU22 diagnostic ultrasound scanner (Phillips Medical Systems, Bothell, WA, USA) were used to image the livers. First the livers were evaluated for the presence of any anatomical abnormalities and air using the L12 – 5 linear array in B-mode imaging and in a contrast mode to ensure uniform perfusion across the whole liver.

The L9 – 3 probe was held fixed in a position using a mechanical arm (**Fig. 1b**) to monitor the perfusion of that specific region and record contrast image loops (**Fig. 2**). A contrast mode with the following parameters was used: power modulation, frequency = 3.1 MHz, MI = 0.05, focus of 3.5 cm, frame rate = 12 Hz, persistence off, and compression maximum (50 dB). The 2 D gain was continuously adjusted and recorded when the intensity-concentration relationship was under investigation, to avoid signal saturation which would result in inaccuracies in the quantification parameters [21]. The image plane was chosen such that it contained a cross-sectional view of each input vessel (PV and HA), a branch of the HV, and well-perfused parenchyma **Fig. 3a – c**.

## Flow protocol

Two specific tasks were studied in each of the 3 livers:

1. The effect of bubble concentration on quantification parameters (*RT*, *MTT*, *AUC*, *PI*) under constant flow.
2. The effect of flow changes in the HA and PV on bolus quantification parameters measured on the macro-circulation, the micro-circulation in the parenchyma, and the HV vascular tree.

In task (2), 3 different flow changes were considered as outlined in **Table 1**. Flow Changes A allowed for changes in both the HA and the PV while the overall total flow remained constant. In Flow Changes B, the PV was held constant while the HA was varied and thus the overall total flow was varied. Similarly in Flow Changes C, the HA was held constant while the PV was varied and thus the overall total flow was varied.

For task (1), a total of 8 microbubble solutions were prepared using the following dilutions (mL added in 1 L): 0.1665, 0.0908, 0.0196, 0.0099, 0.0040, 0.0020, 0.0010, and 0.0005. The concentrations that were used cover a clinically relevant wide range. Since the bolus is going directly to the liver, it is diluted in a lot less fluid compared to an intravenous bolus injection in-vivo. We have assumed that while for a patient the bolus is spread in 5 L of blood, the bolus is diluted in 0.5 – 1 L of total fluid (in the actual liver) in the machine-perfused liver. Thus, the highest dilution (0.1665 ml in 0.5 – 1 L) is not far from the clinical dose (1 ml in 5 L). The measurement time was kept below 1 hour to avoid bubble deterioration. The bolus volume was 1 ml injected through a rubber stop in either the PV or the HA. One-minute video loops were collected for every in-

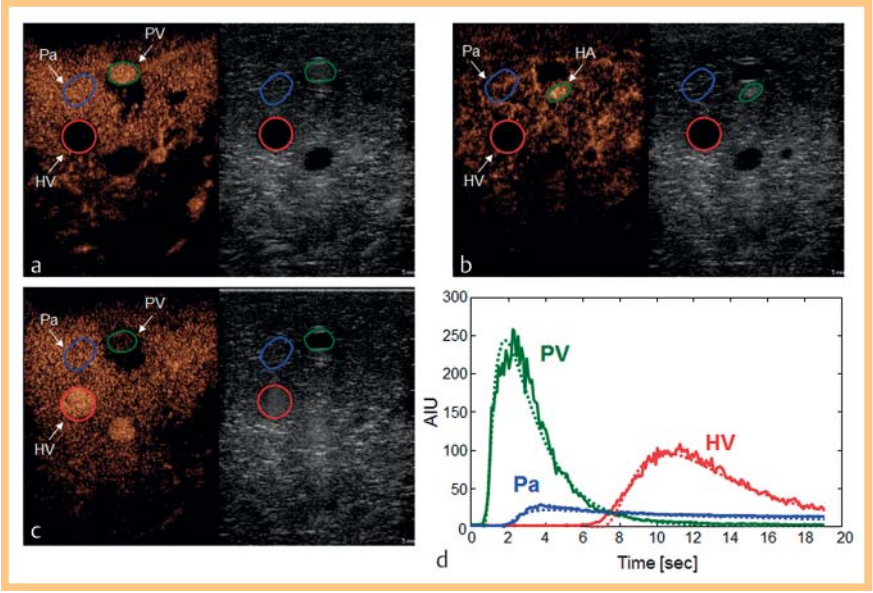


**Fig. 3** **a – c** Images of the liver after bolus injection in the PV **a**,**c**, and the HA**b**. **a** and **c** are from the same image loop but at different times. Three ROIs were placed on each image: one around the input vessels [the portal vein (PV) or the hepatic artery (HA)], one around the output vessel [hepatic vein (HV)] and one in an area of well perfused parenchyma (Pa). **d** Typical time-intensity curves (TICs) for portal vein, hepatic vein and parenchyma. The formed TICs are shown in solid lines and the LDRW model fit is shown in dashed lines.

**Table 1** List of flow variations induced in the perfusion system. Three different cases were studied. Flow Changes A: The total flow rate was kept constant while both the PV and the HA flow rate were changing to maintain the total flow rate at 1200 ml/min. Flow Changes B: The PV flow rate was kept constant while the HA flow rate was changing. Flow Changes C: The HA flow rate was kept constant while the PV flow rate was changing.

| Flow Changes A | | | Flow Changes B | | | Flow Changes C | | |
|---|---|---|---|---|---|---|---|---|
| PV (ml/min) | HA (ml/min) | Total flow (ml/min) | PV (ml/min) | HA (ml/min) | Total flow (ml/min) | PV (ml/min) | HA (ml/min) | Total flow (ml/min) |
| 800 | 400 | 1200 | 1000 | 400 | 1400 | 1400 | 200 | 1600 |
| 850 | 350 | 1200 | 1000 | 350 | 1350 | 1200 | 200 | 1400 |
| 900 | 300 | 1200 | 1000 | 300 | 1300 | 1000 | 200 | 1200 |
| 950 | 250 | 1200 | 1000 | 250 | 1250 | 800 | 200 | 1000 |
| 1000 | 200 | 1200 | 1000 | 200 | 1200 | 600 | 200 | 800 |
| 1050 | 150 | 1200 | 1000 | 150 | 1150 | 400 | 200 | 600 |

jection. Between injections, a C5 – 1 curve linear array probe was used to destroy any remaining microbubbles in the system.

In order to study the ability of DCEUS quantification to detect flow changes in the liver vasculature, flow changes at the PV or the HA or both were induced via the flow regulators. These clinically relevant flow rates (**Table 1**) mimic in a simplified and controlled manner flow changes that might be caused during the progression or regression of tumor angiogenesis. Bolus injections of 1 ml and contrast concentration of $C = 0.1‰$ were used and 1-minute loops were collected. A new vial of contrast agent was used for the whole set of flow variation measurements. The experiments were repeated in a total of 3 livers and results are shown as the mean ± standard deviation. In order to combine parameters from different livers, which also meant different ROIs and different vasculature, the extracted quantification parameters were normalized with respect to the maximum value of each parameter in every liver.

## Contrast agent

Custom-made microbubbles (Department of Pharmaceutics, University of Ghent, Ghent, Belgium), very similar to Definity (which was not available in our country), clinical ultrasound contrast agents were used in this work. Microbubbles were prepared as described in [22]. The average size of the microbubbles was 2.5 µm and they contained Perfluorobutane gas (PFB, $C_4F_{10}$). The concentration of the microbubbles was $3 – 8 \times 10^8$ microbubbles/mL.

## Image quantification

QLAB software (Philips Medical Systems, Bothell, WA) was used to form TICs from the DICOM files by placing an ROI on the image (**Fig. 3a–c**). TICs of both input vessels (PV or HA), the output vessel (HV) and the parenchyma (Pa) were extracted from QLAB (**Fig. 3 d**, solid lines)) and were fitted to an LDRW model (**Fig. 3 d**, dashed lines)]. DCEUS quantification parameters, *RT*, *MTT*, *AUC* and *PI*, were extracted from the fitted model.

## Results

The effect of bubble concentration on quantification parameters under constant flow is shown in (**Fig. 4a – f, g – l**) for injections at the PV and HA, respectively, in a semi-log scale to better accommodate the large range of concentrations used. It is observed that *RT* remains constant with increasing concentration both in larger vessels of the PV, HA and HV and micro-circulation (Pa) (**Fig. 4a – c, g – i**). This result was expected as the

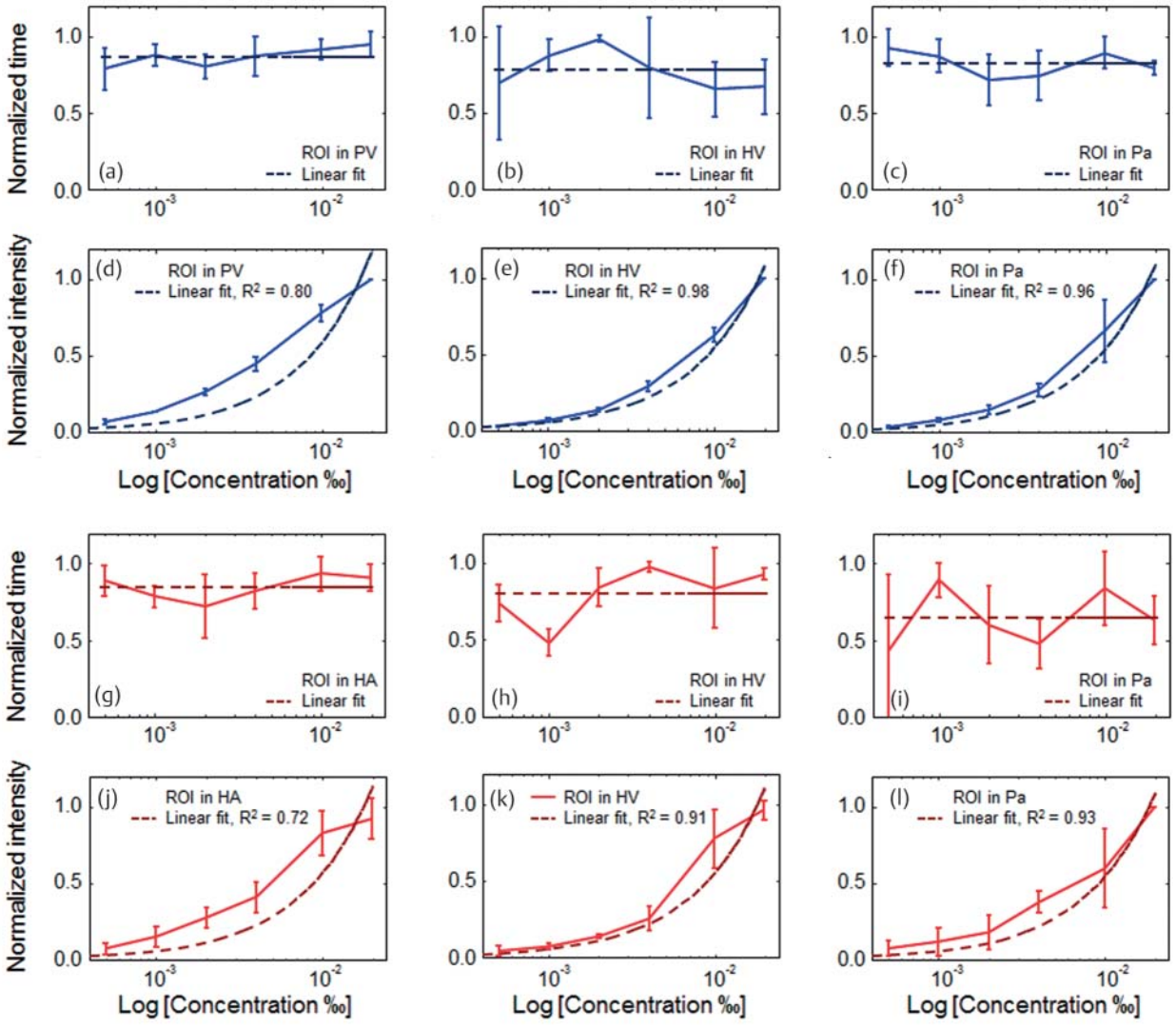


**Fig. 4** **a–c** Normalized rise time **a–c, g–i** and normalized peak intensity **d–f, j–l** as a function of bubble concentration in semi-log scale after a PV and an HA bolus injection, respectively. PV injection is shown as a blue line and HA injections are shown as a red line. **a, d, g, j** ROI on a PV or on an HA main vessel, **b, e, h, k** ROI on an HV main vessel, **c, f, i, l**) ROI on the parenchyma. A straight line (y = constant for RT and y = x for PI) was fitted in the data and it is shown in dashed lines.

flow rate was kept constant in these measurements [see Eq. (2)]. However, it is observed that *PI* increases linearly with increasing concentration (**Fig. 4d–f, j–l**), which is expected and in agreement with previously published results [9, 21]. A straight line was fitted in the data to make it easier for the reader to appreciate the linear relationship in a semi-log scale. The quality of fit is excellent with $0.72 < R^2 < 0.96$. The deviations of *PI* from the linear fit are attributed to the increased acoustic shadowing (higher attenuation at higher microbubble concentrations) [21]. Thus, the two higher concentrations were omitted from the plots.

**Fig. 5** shows the normalized *RT* as a function of flow rate for the case where the total flow rate was kept constant at 1200 ml/min (**Table 1,** Flow Changes A). It is observed that the normalized *RT* decreases when the flow rate increases in both large vessels, the HA (**Fig. 5a**) and the PV (**Fig. 5 d**). However, the *RT* change in HA is more pronounced than in the PV because the induced flow rate change in the HA was greater (from 150 to 400 ml/min, 2.7x) than in the PV (from 800 to 1050 ml/min, 1.3x). The measurements in **Fig. 5a, d** are fitted with $1/Q$ curve and shown as a dashed line, with $R^2 = 0.93$ and $R^2 = 0.90$, respectively. In the HV (**Fig. 5b, e**) it is observed that *RT* does not follow a specific trend with increasing flow rate in both arterial and venous injections. This result is attributed to the fact that the HV reflects the summation of PV and HA flows, which is kept constant at 1200 ml/min in this case. For the same reason, in the parenchyma after injection in the HA (**Fig. 5c**) and the PV (**Fig. 5f**), despite the induced flow rate change, the *RT* still stays constant.

The case where flow rate changes were induced only in the HA tree while the flow rate of the PV vasculature was maintained constant (**Table 1,** Flow Changes B) is shown in **Fig. 6a–c**. It is observed that these flow rate changes are detected in the input vessel as *RT* decreases with increasing flow rate (**Fig. 6a**), but not in the HV vessel, **Fig. 6b**, or the microcirculation in the par-

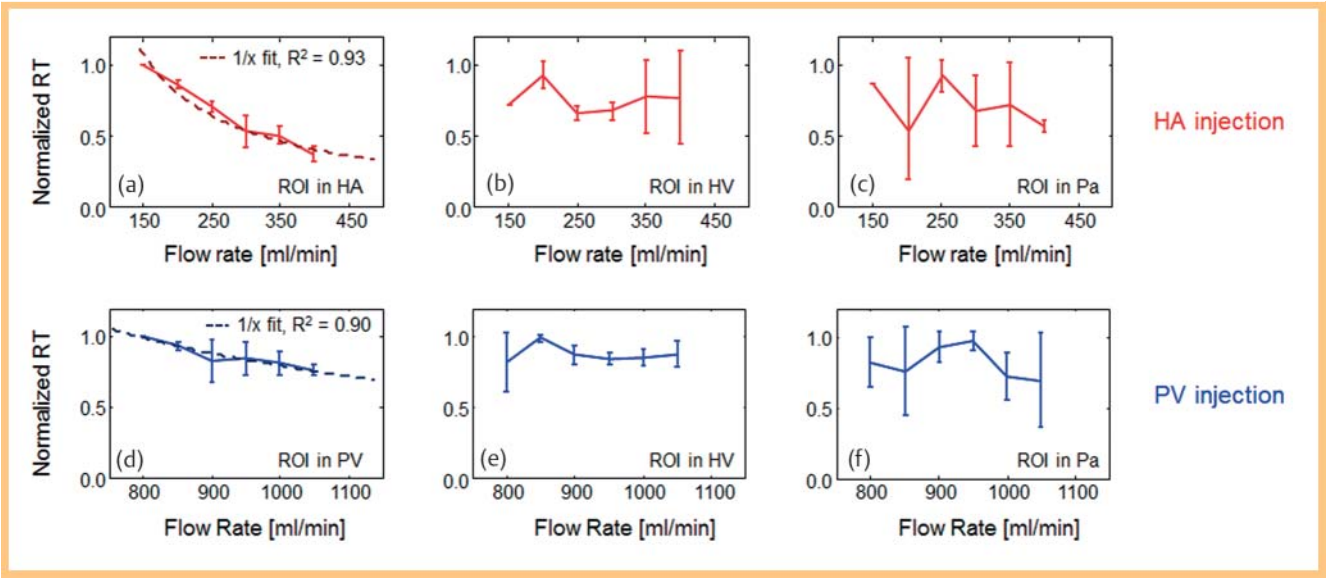


**Fig. 5** Flow Changes A. Normalized rise time (RT) as a function of flow rate. Top row: bolus injections in the hepatic artery; bottom row: bolus injections in the portal vein. The total flow rate was kept constant at 1200 ml/min while both the portal vein and the hepatic artery flow rate were changing. A 1/x curve (y = a/x) was fitted in the data and it is shown in dashed lines.

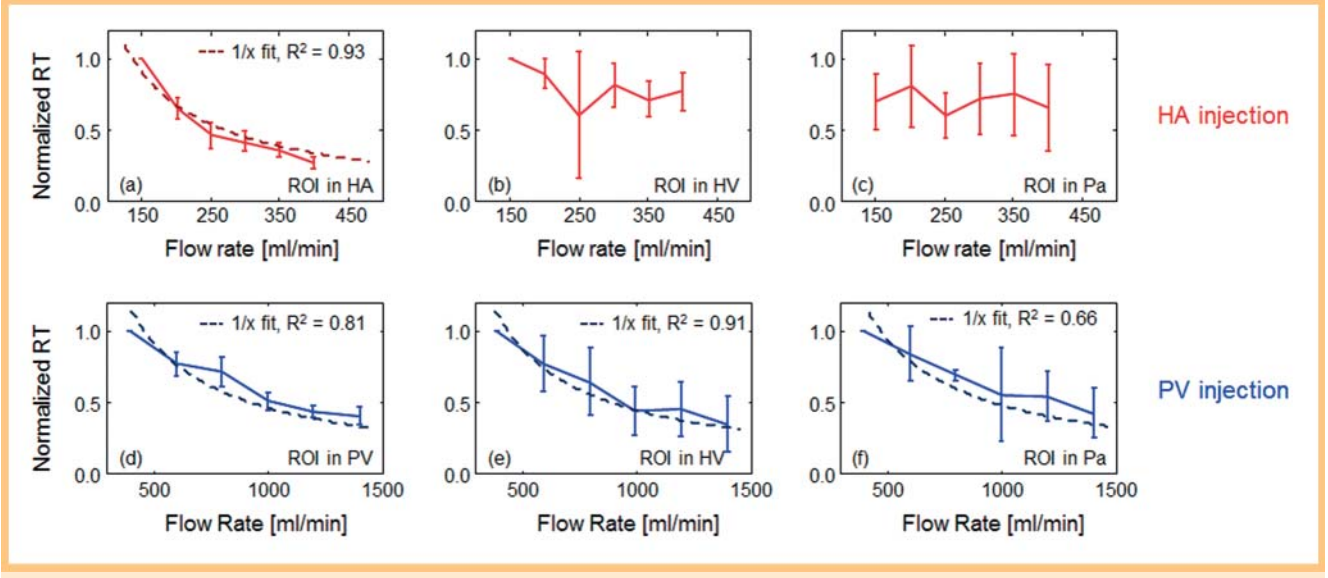


**Fig. 6** Normalized rise time (RT) as a function of flow rate. Top row: bolus injections in the hepatic artery. Portal vein flow was kept constant at 1000 ml/min while the hepatic artery flow was changing between 150 – 400 ml/min (**Table 1**, Flow Changes B). Bottom row: bolus injections in the portal vein. Hepatic artery flow was kept constant at 200 ml/min while the portal venous flow was changing between 400 – 1400 ml/min (**Table 1**, Flow Changes C). A 1/x curve (y = a/x) was fitted in the data and it is shown in dashed lines.

enchyma, **Fig. 6c**, as no clear trends or significant changes of *RT* with increasing flow rate are observed. **Fig. 6d – f** show *RT* for the case where flow rate changes were induced in the PV while the HA flow rate was kept constant (**Table 1,** Flow Changes C). It is observed that *RT* decreases with increasing flow and the induced flow rate changes are reflected in the *RT* of both the input (**Fig. 6 d**) and the outflow vessel (**Fig. 6e**) and also can be detected in the micro-vasculature (**Fig. 6f**). Since the outflow vessel (HV) reflects the summation of PV and HA flows and taking into account that approximately 75 % of the total flow is supplied by the PV, the outflow is only minimally affected by the changes in the arterial vascular tree when PV flow is kept constant (**Fig. 6b**). Thus, the changes induced in the HA (**Table 1,** Flow Changes B) cannot be measured from the quantification parameters extracted from the TICs.

**Fig. 7** shows *AUC* as a function of flow rate for Flow Changes B **Fig. 7a – c** and Flow Changes C (**Fig. 7d – f,** **Table 1**). The trends in **Fig. 7** are similar to those of **Fig. 6**. Specifically in **Fig. 7a-c** where flow rate changes were induced only in the HA, the flow changes could be detected only in the input vessel (**Fig. 7a**). *AUC* decreases with increasing flow rate according to Eq. (2). In **Fig. 7d – f** where flow rate changes were induced only

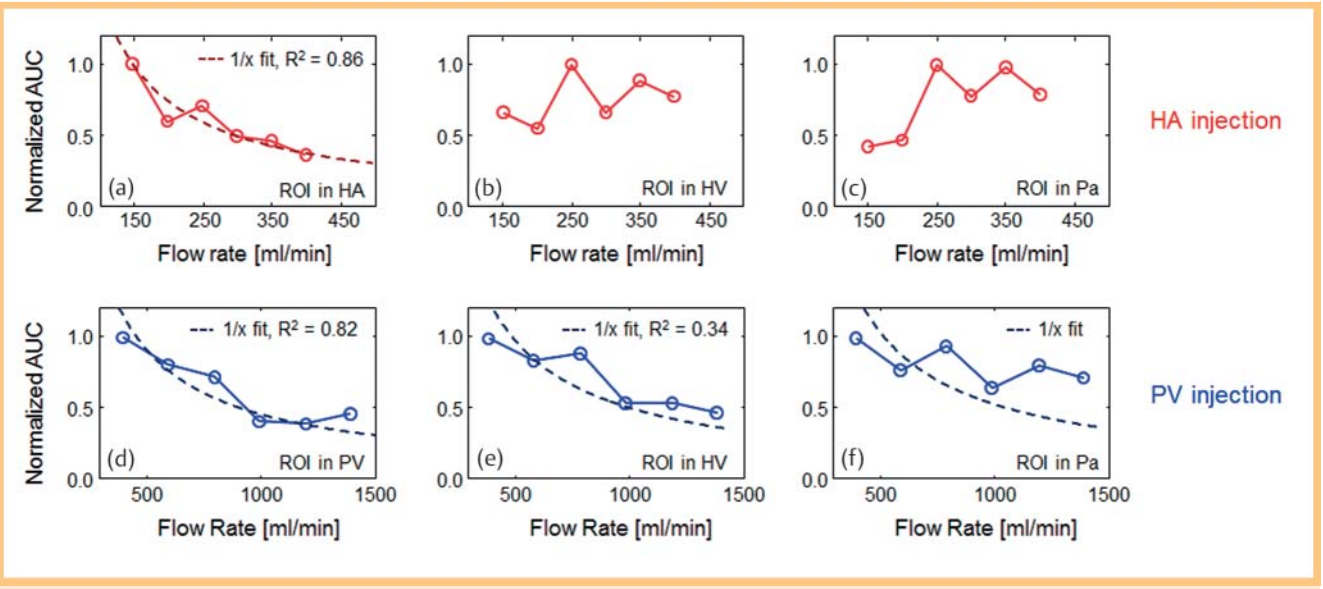


**Fig. 7** Normalized area under the curve (AUC) as a function of flow rate. Top row: bolus injections in the hepatic artery. Portal vein flow was kept constant at 1000 ml/min while the hepatic artery flow was changing between 150 – 400 ml/min (**Table 1**, Flow Changes B). Bottom row: bolus injections in the portal vein. Hepatic artery flow was kept constant at 200 ml/min while portal venous flow was changing between 400 – 1400 ml/min (**Table 1**, Flow Changes C). A 1/x curve (y = a/x) was fitted in the data and it is shown in dashed lines.

in the PV, it is observed that *AUC* decreases with increasing flow both in the input (**Fig. 7 d**) and the outflow vessel (**Fig. 7e**), as well as the parenchyma (**Fig. 7f**).

Finally, **Fig. 8a, b** show *PI* as a function of flow rate for Flow Changes B (**Table 1**) and Flow Changes C (**Table 1**), respectively. It is observed that *PI* is relatively constant with flow rate changes for both the input vessels (HA, **Fig. 8a** and PV, **Fig. 8b**). *PI* is expected to change when the vascular density changes which did not change for the healthy livers studied here.

## Discussion

DCEUS has the potential to measure relative flow changes in the microcirculation and this opens the possibility for its use as an imaging biomarker of tumor response to therapy. Despite its existence for over 10 years and a number of published works, there are still some basic questions and issues such as the relationship of the bolus dynamics quantification parameters with flow, its accuracy and resolution, reproducibility, and its limitations. In trying to address some of the issues above, machine-perfused pig liver presents itself as an ideal test bed due to its clinical relevance. One small drawback is that there are no tumor models for such a system, but in-depth understanding of the DCEUS ability to measure flow in the microcirculation in a normal functioning liver is of great importance.

One problem we have encountered is that certain microbubbles may be sticking in the pig liver microvasculature [20]. Sonovue (Bracco S. P. A., Milan, Italy) was also used (results not shown here) and very similar trends were observed with the exception that some sticking to the microcirculation was observed. The microbubbles currently in clinical use do not have any similar "sticking" issues reported in humans. In machine perfusion models the absence of lungs to filter larger microbubbles presents a small problem as larger microbubbles circulate in the liver. How-

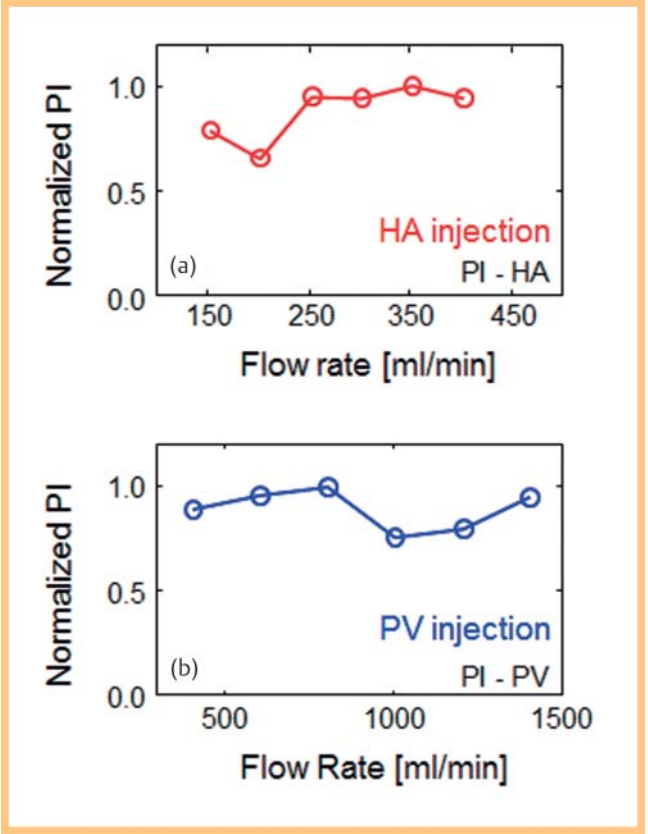


**Fig. 8** Normalized peak intensity (PI) as a function of flow rate. **a** Bolus injection in the hepatic artery. Portal vein flow was kept constant at 1000 ml/min while the hepatic artery flow was changing between 150 – 400 ml/min (**Table 1**, Flow Changes B). **b** Bolus injection in the portal vein. Hepatic artery flow was kept constant at 200 ml/min while the portal venous flow was changing between 400 – 1400 ml/min (**Table 1**, Flow Changes C).

ever, according to the principles of indicator dilution, the size of the microbubbles does not directly affect flow measurements.

The intensity-bubble concentration relationship under low MI conditions was studied for the first time in a clinically relevant model. A linear relationship was confirmed for up to a certain concentration at which acoustic shadowing begins. All errors from signal saturation in the ultrasound scanner were removed by a previously published method [21] of continuous gain adjustment in both the scanner and the quantification software. *RT* and *MTT* are not affected by bubble concentration changes. This is an important result for clinical studies as measurements of flow rates in-vivo from *RT* and *MTT* will not be affected by variation in the concentrations between injections. However, large bubble concentrations should be avoided for accurate quantification of flow.

We have induced a variety of flow changes by virtue of adjusting the pump controlling the flow in both the HA and the PV of the perfused livers and tried to measure the induced changes in the larger vessels of those vascular trees, the HV, and the liver parenchyma. One advantage of the ex-vivo machine perfusion model is that injections to either the HA or the PV are administered and thus those specific vascular networks are studied independently.

In the first set of flow changes (**Table 1,** Flow Changes A) where the overall flow rate was held constant while the HA and the PV were changing proportionally, the change on the specific input vessel (HA or PV) was clearly reflected in terms of *RT* changes. Similar trends were observed with the *MTT* (not shown here) which according to Eq. (2) is proportional to the flow rate. However, flow changes in either the HA and the PV while the overall flow (HA+PV) was held constant should not amount to any flow changes in the HV or the parenchyma which is in agreement with our measurements (**Fig. 5b–c, e–f**). We note here that this type of flow change is perhaps the closest to liver tumors in-vivo. Our findings suggest that tumoral flow changes will best be recorded in the larger arterial vessels and not the parenchyma.

When the total liver flow was allowed to change by changing either the HA flow while keeping the PV constant and vice versa (**Table 1,** Flow Changes B and C), we were able to easily measure these changes in the input vessels (HA or PV) (**Fig. 6a, d**). In the outflow vessel (HV) and the parenchyma, we could detect changes in the *RT* only when the PV flow rate was changed (**Fig. 6e, f**). By considering the overall percent changes in each case, we can deduce the flow resolution of our method. When the HA was changing (**Table 1,** Flow Changes B), the overall flow change was 4 % to 18 % (50/1200 to 250/1400). It is observed that DCEUS quantification may not detect changes in this range in the parenchyma and this may be the lower bound. When the PV was changing (**Table 1,** Flow Changes C), the overall flow change was 25 % to 63 % (200/800 to 1000/1600). In this range of flow changes, DCEUS quantification can detect those changes down to the microvascular level (parenchyma). From these two sets of measurements, we can deduce that DCEUS can effectively measure flow changes when they are about 20 % and above. During the progression or regression of angiogenesis, the resulting flow changes are typically greater than 20 % [23] and thus it would be feasible to measure them with the present technique.

Both *RT* and *AUC* are inversely proportional to the flow rate according to Eq. (2) & (3) and that was confirmed with our results (**Fig. 6 – 7**). In the literature, there is some confusion as to which parameter to use and different investigators suggested using either time (*RT* and *MTT*) or *AUC* for extracting flow information. Their choice was often based on the ability of the ultrasound scanner to accurately measure them or on the statistical correlation of those parameters with other established markers in their experiments. Specifically, single-center studies in patients with metastatic renal carcinoma [16] and hepatocellular carcinoma [15] showed that *AUC* was consistently correlated with RECIST criteria. A multi-center study performed in patients with different types of solid tumors [12] enhanced previous results and showed that *AUC* had the most significant association among other quantification parameters with overall survival. In another clinical trial, a correlation of *RT* with early tumor response to therapy in patients undergoing a combination of antiangiogenic and cytotoxic treatment for colorectal metastasis in the liver was demonstrated [4]. Our work here shows that *RT*, *MTT* and *AUC* are all related to flow. However, measurements performed in clinics may suffer from different sources of error [19]. Generally, intensity parameters (*AUC* and *PI*) are more error-prone due to signal saturation, nonlinear propagation artifact [24], and acoustic shadowing.

Often dramatic changes in both the size and the microvascular flow of tumors take place during chemotherapy, and it becomes even more challenging to accurately measure those changes with 2 D ultrasound due to the inhomogeneous nature of the tumor vasculature. However, our work here shows that it is possible to use DCEUS quantification to monitor those changes, and once 3 D ultrasound technology (imaging and quantification) is clinically available DCEUS quantification will easily be adapted.

One area where DCEUS quantification can play a very important role is monitoring ultrasound-mediated drug delivery approaches like sonoporation [25]. The safety, bedside availability, and relatively low cost of ultrasound, combined with the ability to measure flow in the microcirculation make DCEUS quantification a valuable tool for real-time monitoring of therapeutic applications which target the vascular network of tumors. In addition, machine perfusion of human-sized livers combined with DCEUS quantification may play a pivotal role in the study of tumor ablative techniques such as radio frequency and microwave ablation, cryoablation, and irreversible electroporation where not only the lesion formation may be closely monitored but also the changes in the microcirculation in an area around the ablation zone (penumbra).

In tumor perfusion monitoring where vascular changes are happening either as a result of tumor growth or as a response to chemotherapy, the arterial input to the tumor is changing, thus making it more difficult to accurately apply the techniques described. Changes due to the cardiac output of the patient as a result of possible cardiotoxicity of chemotherapy which also further influence the arterial input function also add to this effect. Thus, we have refrained from trying to estimate absolute blood flow rates and instead noted relative changes. In addition, estimation of *PI* relating to the vascular volume and vascular density, in combination with time parameters related to flow, would be important in those cases despite the fact that amplitude parameters (*PI* and *AUC*) are more prone to signal saturation and acoustic shadowing errors.

## Conclusion

Ex-vivo machine-perfused pig liver is an excellent test bed for DCEUS quantification approaches for measuring flow in the liver vasculature. It allows for precise control of flow rate changes and the study of the HA and PV vascular networks. The intensity-bubble concentration relationship was found to be linear, whereas *RT* and *MTT* are not affected by bubble concentration changes. In-

duced flow changes in the livers were detected both in the larger vessels (HA or PV) depending on where the injection was administered, and in the HV and the parenchyma. DCEUS quantification can detect relative flow changes greater than 20 % everywhere in the liver vasculature.

## Acknowledgement

This work was co-funded by the European Regional Development Fund and the Republic of Cyprus through the Research Promotion Foundation (Project: DIDAKTOR/0311/78). Ine de Cock and Ine Lentaker from University of Ghent are gratefully acknowledged for microbubble preparation used in this work. We are also grateful to Kypros Stylianou for his invaluable technical assistance.

## References

1 *Cosgrove D*, *Lassau N*. Imaging of perfusion using ultrasound. Eur J Nucl Med Mol Imaging 2010; 37 (Suppl 1): S65 – S85
2 *Wilson SR*, *Burns PN*. Microbubble-enhanced US in body imaging: what role? Radiology 2010; 257: 24 – 39
3 *Dietrich CF*, *Averkiou MA*, *Correas JM et al.* An EFSUMB introduction into Dynamic Contrast-Enhanced Ultrasound (DCE-US) for quantification of tumour perfusion. Ultraschall in Med Stuttg Ger 1980 2012; 33: 344 – 351
4 *Averkiou M*, *Lampaskis M*, *Kyriakopoulou K et al.* Quantification of tumor microvascularity with respiratory gated contrast enhanced ultrasound for monitoring therapy. Ultrasound Med Biol 2010; 36: 68 – 77
5 *Lassau N*, *Chami L*, *Benatsou B et al.* Dynamic contrast-enhanced ultrasonography (DCE-US) with quantification of tumor perfusion: a new diagnostic tool to evaluate the early effects of antiangiogenic treatment. Eur Radiol 2007; 17: F89 – F98
6 *Leen E*, *Averkiou M*, *Arditi M et al.* Dynamic contrast enhanced ultrasound assessment of the vascular effects of novel therapeutics in early stage trials. Eur Radiol 2012; 22: 1442 – 1450
7 *Strouthos C*, *Lampaskis M*, *Sboros V et al.* Indicator dilution models for the quantification of microvascular blood flow with bolus administration of ultrasound contrast agents. IEEE Trans Ultrason Ferroelectr Freq Control 2010; 57: 1296 – 1310
8 *Zierler K*. Indicator dilution methods for measuring blood flow, volume, and other properties of biological systems: a brief history and memoir. Ann Biomed Eng 2000; 28: 836 – 848
9 *Lampaskis M*, *Averkiou M*. Investigation of the relationship of nonlinear backscattered ultrasound intensity with microbubble concentration at low MI. Ultrasound Med Biol 2010; 36: 306 – 312
10 *Hudson JM*, *Karshafian R*, *Burns PN*. Quantification of flow using ultrasound and microbubbles: a disruption replenishment model based on physical principles. Ultrasound Med Biol 2009; 35 (12): 2007 – 2020
11 *Gauthier TP*, *Chebil M*, *Peronneau P et al.* In vitro evaluation of the impact of ultrasound scanner settings and contrast bolus volume on time-intensity curves. Ultrasonics 2012; 52: 12 – 19
12 *Lassau N*, *Bonastre J*, *Kind M et al.* Validation of dynamic contrast-enhanced ultrasound in predicting outcomes of antiangiogenic therapy for solid tumors: the French multicenter support for innovative and expensive techniques study. Invest Radiol 2014; 49: 794 – 800
13 *Lassau N*, *Lamuraglia M*, *Chami L et al.* Gastrointestinal Stromal Tumors Treated with Imatinib: Monitoring Response with Contrast-Enhanced Sonography. Am J Roentgenol. 2006 Nov 2006; 187: 1267 – 1273
14 *Williams R*, *Hudson JM*, *Lloyd BA et al.* Dynamic microbubble contrast-enhanced US to measure tumor response to targeted therapy: a proposed clinical protocol with results from renal cell carcinoma patients receiving antiangiogenic therapy. Radiology 2011; 260: 581 – 590
15 *Lassau N*, *Koscielny S*, *Chami L et al.* Advanced hepatocellular carcinoma: early evaluation of response to bevacizumab therapy at dynamic contrast-enhanced US with quantification–preliminary results. Radiology 2011; 258: 291 – 300
16 *Lassau N*, *Koscielny S*, *Albiges L et al.* Metastatic renal cell carcinoma treated with sunitinib: early evaluation of treatment response using dynamic contrast-enhanced ultrasonography. Clin Cancer Res Off J Am Assoc Cancer Res 2010; 16: 1216 – 1225
17 *Aglietta M*, *Regge D*. Response to Treatment: The Role of Imaging. In: Imaging tumor response to therapy. Springer: 2012: 15 – 40
18 *Gauthier TP*, *Averkiou MA*, *Leen ELS*. Perfusion quantification using dynamic contrast-enhanced ultrasound: the impact of dynamic range and gain on time-intensity curves. Ultrasonics 2011; 51: 102 – 106
19 *Tang M-X*, *Mulvana H*, *Gauthier T et al.* Quantitative contrast-enhanced ultrasound imaging: a review of sources of variability. Interface Focus 2011; 1: 520 – 539
20 *Izamis M-L*, *Efstathiades A*, *Keravnou C et al.* Dynamic contrast-enhanced ultrasound of slaughterhouse porcine livers in machine perfusion. Ultrasound Med Biol 2014; 40: 2217 – 2230
21 *Keravnou C*, *Mannaris C*, *Averkiou M*. Accurate measurement of microbubble response to ultrasound with a diagnostic ultrasound scanner. IEEE Trans Ultrason Ferroelectr Freq Control 2015; 62: 176 – 184
22 *De Temmerman ML*, *Dewitte H*, *Vandenbroucke RE et al.* mRNA-Lipoplex loaded microbubble contrast agents for ultrasound-assisted transfection of dendritic cells. Biomaterials 2011; 32: 9128 – 9135
23 *Vaupel P*, *Kallinowski F*, *Okunieff P*. Blood flow, oxygen and nutrient supply, and metabolic microenvironment of human tumors: a review. Cancer Res 1989; 49: 6449 – 6465
24 *Thapar A*, *Shalhoub J*, *Averkiou M et al.* Dose-dependent artifact in the far wall of the carotid artery at dynamic contrast-enhanced US. Radiology 2012; 262: 672 – 679
25 *Lentacker I*, *De Cock I*, *Deckers R et al.* Understanding ultrasound induced sonoporation: definitions and underlying mechanisms. Adv Drug Deliv Rev 2013